Contents lists available at http://qu.edu.iq

Al-Qadisiyah Journal for Engineering Sciences

Journal homepage: https://qjes.qu.edu.iq

A comparative study of radiation models in spray combustion

Alaa Jasim Alshablawi* * and Ahmed Abed Al Kadhem Majhool*

Mechanical Engineering Department, College of Engineering, University of Al-Qadisiyah, Iraq.

ARTICLEINFO

Article history:
Received 15 September 2022
Received in revised form 02 January 2023
Accepted 01 February 2023

Keywords:
Radiation
P1
Spray
Combustion
Model

ABSTRACT

This work deals with the investigation of radiation models for combustion spray. The n-pentane fuel C5h12 is used for chemical reactions with the air. The main objective of these simulations is to compare the experimental data and radiation models for spray combustion and to select the best radiation model. The model is used to interpret the structure and properties of the prediction for spray combustion. The simulated cases are carried out using Ansys Fluent. The mixture fracture probability density function is used to evaluate the non-premixed combustion of vaporized fuel droplets. The Radiation models (p1, discrete coordinate, surface to surface, and Roseland) are used to predict local properties in two dimensions. The results of the numerical simulation are compared with the experimental data. The results showed that the p1 radiation model provides good results through temperature, turbulence kinetic energy, and velocity components.

1. Introduction

In combustion systems with high temperatures thermal radiation is a crucial form of energy transfer that should be taken into account for both basic comprehension and practical application in combustion systems. Liquid-fueled rocket engines, gas turbines, diesel engines, and a fireplace are examples of useful combustion systems. A special care is required to the spray combustion issue. It involves complex processes like evaporation, droplet collision, secondary Breakup, and interaction with turbulences. Radiation, chemical reaction, and turbulent mixing are all instances of this mechanism. As a result, in addition to being one of the hardest processes to mathematically characterize it is also a vital topic that we must study for its many potential applications. The significance of radiation-related difficulties has increased in a variety of engineering models involving high-temperature systems. Along with chemical reaction and radiative active medium, a topic, in particular, must be taken into consideration in combustion engineering. It has properties that are directly tied to gases or particles that are emitting, emitting light, and scattering light. The radiative transfer equation (RTE) is commonly represented in a highly nonlinear integral differential form. Numerical theoretical to study radiative transfer, models, and experimental methods have been developed. [1, 2]. Trivic [3] analyzed the impact of the number of gray gases, angular discretization in the polar and azimuthal directions, and spatial rectangular grids on accuracy. Additionally, a new set of predictions is made for a combination of 0.8 nitrogen, 0.1 water vapor, and 0.1 carbon dioxide as a basis to eliminate the shortcomings of spectral lines and band models. The aim study was to develop a 3-D non-gray gas mathematical model and radiation computer code using the connection of FVM and the weighted sum of gray gases model, which was simple to implement within CFD simulations. Trivic et al [4] used the radiative transfer equation was solved by the discrete ordinates technique and the Legendre polynomial expansions were utilized to assess the scattering phase function.

* *Corresponding author.*
E-mail address: alaajasim797@gmail.com (Alaa Jasim Alshablawi)

https://doi.org/10.30772/qjes.v16i1.900

Nomenclature

Cp	specific heat (J kg^{-1} K^{-1})
g_i	gravitational acceleration (m s^{-2})
k	thermal conductivity (W m^{-1} K^{-1})
p	Static pressure (kg m^{-1} s^{-2})
Pr	Prandtl number
T	Temperature (K)
U_i	velocity (m s^{-1})
S_m	mass to gas-phase (kg m^{-3})
U_p	Droplets velocity (m s^{-1})
F_i	momentum force (kg m^{-2} S^{-2})
h_i	Enthalpy
j_i	diffusion flux (kg m^{-2} S)
r_t	turbulent prandtl number
S_h	volumetric heat source (kg m^{-2} S)
S_f	momentum source term (kg m^{-2} S^{-2})
S_G	Radiation source
K	turbulent kinetic energy
f	mixture fraction

Greek symbols

σ_s	scattering coefficient
σ	Stefan-Boltzmann Constant
$\sigma_{S\lambda}$	spectral scattering coefficient
a_λ	spectral absorption coefficient
Φ_v	Rayleigh dissipation function (kg m^{-3})
μ	molecular viscosity (kg $m^{-2}s^{-2}$)
$\in$	turbulence dissipation rate
G_λ	spectral incident radiation
$S_{G\lambda}$	defined source term

Subscripts

CFD	Computational Fluid Dynamics
DOM	Discrete Ordinate Method
RTE	Radiation Transfer Equation
WSGGM	Weighted Sum Of Gray Gases Model
P1	Spherical Harmonic
PDF	Probability Density Function

The solid particles of different coals and ash were subjected to the new model, and a series of 2-D predictions were made. The effects of the particle size parameter and scattering on the radiative heat flux were examined. The generated model was proven extremely accurate, making it appropriate for expansion towards (i) 3-D geometries, (ii) mixes of non-gray gases with particles, and (iii) incorporation in computational fluid dynamics codes As illustrated by Sun et al [5]. In spherical flame modeling, radiation heat transfer is crucial for predicting the flame speed, among other things. While little research has been done on the one-dimensional non-gray radiation heat transfer in spherical coordinates, it is advantageous to utilize the one-dimensional model to tackle the three-dimensional issues with spherical symmetry. The accuracy of the discrete ordinates' technique and the non-gray P1 approach are studied and contrasted. Results indicate that, with the exception of gas mixing situations, the P1 method's accuracy is comparable to DOM. This essay serves two purposes. The reference solution will be produced using the DOM and the SNBCK model. In terms of the radiative heat source, the P1 model's and WSGG models' accuracy will be examined. Yin [6] studied radiant heat transfer is one of the biggest problems with oxy-fuel, and combustion in oxy-fuel is very different from combustion in an air-fuel fire. A large-scale utility boiler's oxy-fuel combustion of natural gas. A large-scale utility boiler's oxy-fuel combustion of natural gas is numerically investigated. In comparison to the non-gray implementation, the oxy-fuel WSGGM's gray calculation notice ably overestimates the radiative heat transfer to the furnace walls and underestimates the gas temperature at the furnace exit plane, leading to a higher rate of incomplete combustion. Gamil et al [7], analyzed heat transmission within the combustion chamber as thermal radiation. Which has a direct impact on temperature distributions at the combustor walls. This research thoroughly analyzes the effects of two radiation models on the temperatures of the flame and liner walls. The results showed that the use of radiation models reduces the flame peak temperature and changes the distribution of temperature throughout the liner. The Discrete Ordinates Approach predicted a temperature at the front of the liner that was 15% lower than the P-1 radiation method and 10% higher than the non-radiation model. Additionally, for the DOM and P-1 cases, respectively, the radiation models underestimated the flame temperature by 200 K and more than 200 K. The findings also indicated that the emissivity value had no impact on the distribution of combustor temperature. Baek et al [8].

Used the discrete ordinate method (DOM) to account radiative transfer equation and the weighted sum of gray gases model (WSGGM). The findings indicate that, when using the non-grey gas model, the total burning time increases because of a reduction in the total heat flux. Additionally, it is discovered that the radiative loss to the outside environment is higher for the non-gray scenario, lowering the maximum gas temperature and flame thickness. Consequently, utilizing a non-ray gas model could lead to greater agreement with experimental data. Hjärtstam et al [9]. Used propane-fueled air and oxy-fuel fires using computational fluid dynamics. Investigated the emission of gas and soot-related radiation processes. In oxy-fuel combustion, CO2 and H2O take the role of N2 in air combustion. Consequently, the radiative heat transmission characteristics of the combustion atmospheres differ. Additionally, oxy-fuel flames vary from air-fired flames in their soot formation properties. Both gas-related radiation and soot-related radiation must be considered when modeling temperature and heat transfer conditions since both may be essential for the design of oxy-fuel furnaces. The investigation's goal is to assess how combustion gases and soot impact flame heat and transfer models. Both gray and non-gray methods are used to account for the gas radiation to see whether a gray model is sufficient to provide a reliable solution when used in CFD simulations of oxyfuel burning [10]. Gray radiation modeling in one dimension in comparison to non-gray radiation modeling in pure water and carbon dioxide as the medium conditions. His study demonstrated the need for high-fidelity models to be used in calculations for non-gray radiation by comparing them to line-by-line benchmark data. The comparison of one-dimensional prototype grey radiation modeling and non-grey radiation modeling revealed that the errors that result from using grey models in the calculations depend on the scale of the geometry, the temperature and concentration gradients within the domain, and the thermal boundary conditions. Choi and Beak [11] studied the effect of radiation in a liquid spray combustion chamber. The radiative transfer equation (RTE) and the weighted sum of gray gases model (WSGGM) solved by the discrete ordinates method (DOM) were applied to model a non-gray radiation effect by CO2 and H2O gases. The WSGGM with DOM was achieved by summing RTE solutions for each gray gas. The finding has demonstrated that radiation accelerates the gasification of the droplets. Resulting in shorter droplet trajectories. A higher than usual high temperature was also brought on by the radiation. Within the combustion zone, it was discovered that the radiation effect improved the spray

combustor efficiency. Fordoei and Mazaheri used the IFRF methane-oxygen combustion furnace, the impact of the method for calculating absorption and emission coefficients, and the radiation model [12]. Employed the P1 (spherical harmonic radiation model) and DO (discrete ordinate) models. The absorption and emission coefficients were calculated using constant coefficients. The findings show that in oxy-fuel combustion, failing to account for radiation heat transfer results in a substantial mistake in predicting temperature distributions inside the furnace, including the maximum and average. The DO model is also more accurate than the P1 model, which means that more heat will be lost when the optical thickness is low. Based on numerical simulations, the WSGGM model for computing absorption and emission coefficients produces the best results in comparison to other methods. Frank et al. dveloped a surface-to-surface radiation model to obtain accurate temperature distribution simulation results within the switch cabinets [13]. This model computes net heat flow for flat, gray, and diffuse surfaces at various temperatures. The precision of this computation is heavily reliant on the exact numbers for the radiation view variables. The view factors are calculated using the Monte Carlo approach. Various modifications to grid spacing, photon quantity, and a quasi-Monte Carlo approach are explored. The radiation model is validated using numerical comparison data for a specific size switch cabinet with and without electronic parts within. Hosseini et al [14] Using the ANSYS Fluent CFD simulation, it was determined how the input air swirl number affected the temperature, radiation heat flux distribution, and dynamic flow behavior of a methane-air diffusion flame. We looked at the characteristics of turbulent flow and radiation heat flux. The research revealed that increasing the swirl number of the incoming air from 0.0 to 0.6 causes the internal recirculation zone of the furnace to grow. As a result, the leading high-temperature zones, which are the source of nitrogen oxides, are reduced, increasing the efficiency of combustion and improving the efficiency of the mixture of fuel and air (NOx). The ultimate result is a 58.6 percent reduction in NOx emissions and a 36.5 percent improvement in flux radiation efficiency. Krishnamoorthy using traditional iterative techniques, the P1 radiation model's iterative convergence might be sluggish in optically thin circumstances [15]. An internal P1 radiation model was interfaced with high-performance, scalable, linear solver libraries to address this flaw. The accuracy of P1 radiation model calculations was then evaluated by comparing the results of prototypical situations that were representative of contemporary combustion systems to results from discrete ordinate model calculations. When compared to traditional Gauss-Seidel sweeps, the Pre-Conditioners to the Conjugate Gradients approach decreased the convergence time of the P1 radiation model by a factor of 30 for small issue sizes and a factor of 70 for larger problem sizes. Chiu and Chang [16]. They studied the effects of radiation on the rate of burning and droplet vaporization. They assumed the atmosphere surrounding the droplet is quiet, and the polarization and the burning processes remain constant. The examination of vaporization, vapor, and combusting droplets. The ambient temperatures range from 500 K to 2500 K, while the droplet sizes range from 10 PM to 250 PM. It has been discovered that a droplet's rate of vaporization grows with droplet size and ambient temperature and may be 400% more than the rate of non-radiative gasification, although, with a slower trend, the combustion rate of a droplet rises together with droplet size and ambient temperature. Crnjac et al [17], studied the Navier-Stokes equation and the P1 radiation models and Rosseland in the context of the boundary element method. The validity of the proposed implementation is assessed using a test in one dimension using a participant medium of grey in radiative equilibrium between two surfaces of black that are isothermal. Radiation's impact on overall heat transport is explained by the energy equation. In addition to the diffusion heat flux, the radiative heat flux also has to be taken into account. This is done in such a manner that the energy equation has a term for the divergence of the radiative flow vector. An important problem in computational fluid dynamics is the radiative transfer equation (RTE), an integro-differential equation. Applying the selected radiation model results in a simplification of the radiative transfer equation under the specified physical conditions. In this study, the P1 approximation and the Rosseland diffusion approximation are used to illustrate the contributions from radiant energy transmission for optical thick fluids. Juri et al [18]. Studied the effect radiative heat transfer has on compression ignition engines operating at high temperatures, which also has an impact on the way pollutants are formed, user functions are added to the AVL FIRETM CFD system, and the discrete ordinates method using the finite volume method. Results show the reduced peak temperatures of around 10 K led to concentrations of nitrogen oxides that were about 18% lower and soot concentrations that were up to 20% higher after the engine working cycle. At crank angles, radiative heat transmission has the most noticeable effect on soot development. It can be said that the combination of models that have been put into practice helps predict the heat transfer of internal combustion engines with a focus on radiative heat transport, which can be a crucial aspect in the development of upcoming internal combustion engines. Furuhata et al [19], studied is to evaluate the effectiveness of numerical spray combustion modeling. It is discussed how to use a numerical simulation to estimate the local characteristics of heavy oil spray flames stabilized by a baffle plate. To estimate the combustion gas flow, gas composition, and temperature fields in the experimental combustor, time-averaged governing conservation equations are solved. The Lagrangian approach is used to predict how fuel droplets would behave in a turbulent combustion gas flow. The eddy dissipation model calculates the fuel vapor combustion rate. By comparing the simulation's output to measurable data, the simulation's performance is evaluated. By contrasting the estimated and measured findings, the simulation's accuracy is analyzed and presented. Yue and Reitz [20]. Studied computational analysis of internal combustion engine radiative heat transfer. Internal combustion engine radiative heat transport is investigated using computational fluid dynamics models. A typical diesel engine, a compression ignition engine, and current tests for participating gas emissivity and radiative heat transfer are used to completely evaluate the integrated model. The findings indicate soot contributes to radiative heat transfer in engine combustion, and the involved gases are the primary source. Radiative heat loss accounts for approximately 9 to 18% of total wall heat loss in the engine scenarios studied, which range from low to high load, and is found to be linearly related to the global equivalency ratio. The addition of the thermal ratio results in an increase in the emission at exhaust valve opening of up to 50%. NOx emissions are less affected by the radiation. Aghanajafi and Abjadpour [21], used the discrete ordinates approach to solve the 2-D radiative transfer problem (RTE). Linear and non-structured grids have been used to examine complicated 2-D geometry. Geometric parameters with straight edges, ad sloping, and curved borders are all taken into account. It is thought of as a participatory medium that absorbs and releases radiation. To mesh the complicated structure with the Cartesian grid, block-off and incorporated boundary processes are utilized. To cope with the intricacy of the borders, an unstructured grid is employed for further accuracy. This work also seeks to solve temperature fields in radiative equilibrium issues with non-continuous heat loads. It is demonstrated that using an unstructured grid to solve RTE is appropriate for all geometries with simple, sloping, and curved bounds. Bellan et al [22], evaluated the thermal performance of a recently designed 5 kW fluidized bed reactor for

solar gasification. The particulate flow was modeled using the discrete element method (DEM), and the multiphase flow was modeled using the CFD approach. Experiments were conducted and compared to modeling findings to evaluate the established model. The radiative transfer equation was solved using the discrete ordinate radiation model. The reactor's thermal performance and particulate flow behavior have been anticipated, and the effects of particle size, particle size distribution, and gas flow rate have been investigated. The results show that once the ring area particles are fluidized, performance improves because the high porosity enhances the rate of diffusion of radiation. Rajhi et al [23], analyzing gas radiation models for oxy-combustion in CFD modeling. The calculation of the radiation energy is crucial. Different gas radiation models. Depending on the application, the accuracy and complexity of these radiation models vary. Using three different combustion conditions, a CFD model for a typical industrial water tube boiler was created in this study. The three combustion conditions are fuel combustion with air (21 percent O2 and 79 percent N2), oxy-fuel combustion (21 percent O2 and 79 percent CO2), and oxy-fuel combustion (27 percent O2 and 73 percent CO2). The findings are relatively close to the experimental data for the current boiler combustion application. The properties of oxygen-fuel combustion were examined and contrasted with those of air-fuel combustion. Watanabe et al [24], studied a numerical simulation of turbulent spray combustion. a jet burner that produces high-velocity, high-temperature jet exhaust fumes. The k-e turbulence model was used to solve momentum and energy. In addition, a six-flux model was used to calculate the radiative heat transfer technique in combination with a WSGGM (weighted sum of gray gases model). They investigated the impact of heat radiation from soot on the environment, where the predicted temperature was higher than the experimental without soot radiation data. In the case of heat radiation from soot, however, there were significant disparities between the calculated and experimental results. Because of this, many studies have looked into the effects of radiation on combustion. However, in the case of turbulent combustion, it is necessary. To best investigate turbulence, radiation, and chemical interactions, as well as precise reaction mechanisms. Bidi [25], used turbulently premixed in an axisymmetric cylindrical methane-air combustion. A second-order finite volume model was used to numerically simulate the chamber. The chemistry of combustion was modeled using a simplified model. There are 16 species and 31 elementary reactions in the mechanism, which includes some C1 and C2-chain species. For three turbulent premixed methane-air flames, all numerical findings were compared to experimental data. Chishty et al [26], employed three different methods: the discrete ordinate method, the spherical-harmonics method, and the optically thin assumption to solve the radiative transfer equation.

The interactions between turbulence, chemistry, soot, and radiation have been captured by coupling the radiation models for soot and turbulent reactive flows using the conveyed probability density function approach. Unresolved turbulent changes in temperature and composition are a part of this technique. Results indicate that compared to soot, the gas phase (mostly CO2 and H2O species) contributes more to the net radiative heat transfer. The impact of radiation absorption was shown to be significant, and it was discovered that the average radiation time scale overlapped with the lengthy injection period, having a modest impact on temperature distribution. Radiation has little impact on the flame lift-off length, and tiny variations in soot generation are noticeable. The DOM and P1 versions' performance is comparable, however, the optically thin hypothesis amplifies the cooling impact. It is anticipated that radiative heat transfer would have a more noticeable impact on NOx generation rates. The investigation of the radiation effect's function in a spray combustion system is the primary goal of this work. comparison between radiation models (p1, discrete coordinate, surface to surface, and Roseland). Different parameters, such as static temperature, velocity components of the gas phase, mass fraction of CO2, mass fraction of H2O, and turbulence kinetic energy, are used to study how four different radiation models are used to simulate spray combustion.

2. Mathematical Modelling

2.1 Gas-Phase

The governing equations for the Eulerian multiphase are continuity, momentum, and energy conservation equations. It deals with phases individually and models the gas phase as a continuum. For each phase in the system, the mass conservation equation is applied. When a process begins, the model only considers the gas phase, not the interaction of two phases. The source term is acquired once the particle's trajectories have been solved. With the addition of the source term to the equation, ANSYS FLUENT resolves the gas phase.

$$\frac{\partial}{\partial x_i}(\rho u i) = S_m \tag{1}$$

Where: u_i is the component of the air velocity in the continuous phase(m⁄s), and S_m is the increment of the mass to the gas-phase from liquid-phase in (kg⁄m^3). Each phase's momentum equation is solved independently, momentum is transferred between the two phases, and each phase shares a single pressure.

$$\rho u_i \frac{\partial ui}{\partial xi} = \frac{\partial}{\partial xj}\left[\mu\left(\frac{\partial ui}{\partial xj} + \frac{\partial uj}{\partial xi}\right) - \frac{2}{3}\mu(\frac{\partial uj}{\partial xj})\delta ij\right] + \rho g i - \frac{\partial p}{\partial xi} + Sf \tag{2}$$

Where the momentum source term is S_f in (kg⁄m^2 s^2), the gravity is g_i in (m⁄s^2), a molecular viscosity μ is in (kg⁄m^2 s^2)

$$\rho u i \frac{\partial e}{\partial xi} = -p\frac{\partial ui}{\partial xi} + \Phi v + \frac{\partial}{\partial xi}\left(k\frac{\partial T}{\partial xi}\right) + \frac{\partial}{\partial xi}(\sum_{i=1}^{n} h_i J_i) + S_h \tag{3}$$

Where the static pressure is p in (Pa), the momentum force is S_h in (kg ⁄ (m^2, S^2)), the Rayleigh dissipation function is Φ_v in (kg⁄m^3), the thermal conductivity is K in (W/m.k), the air temperature is T in (k), the enthalpy for a specific Phase i is hi, the diffusion flux at a specific phase is J_i in (kg⁄m^2 s), the volumetric heat source is S_h in (kg⁄(S^3 m)).
The conservation equation for predicting the local mass fraction for each phase:

$$\rho u i \frac{\partial mi}{\partial xi} = -p\frac{\partial J_i}{\partial x_i} + S_m \tag{4}$$

$$J_i == -\rho D_{i,m}\frac{\partial m_i}{\partial x_i} \tag{5}$$

Where: the local mass fraction of species phase is m_i, and the diffusion coefficient for species phase in the mixture D_(i,m).

2.2 Turbulence modelling

In practical and technological applications, there is a mathematical representation of turbulence called turbulent flow. The turbulence model was utilized to forecast the alteration of the turbulence using simple equations.

2.2.1. Standard k-∈ modelling

The Standard model derivation ignores the effects of molecular viscosity and assumes that the flow is totally turbulent. It is only suitable for completely turbulent. According to their respective values for the kinetic energy k and ∈ turbulence dissipation rate:

$$\frac{\partial}{\partial t}(\rho k)+\frac{\partial}{\partial x_i}(\rho k u_i)=\frac{\partial}{\partial x_j}\left[(\mu+\frac{\mu_t}{\sigma_k})\frac{\partial k}{\partial x_j}\right]+G_k+G_b-\rho\epsilon-Y_m+S_k \quad (6)$$

$$\frac{\partial}{\partial t}\rho\epsilon+\frac{\partial}{\partial x_i}(\rho\in u_i)=\frac{\partial}{\partial x_j}\left[(\mu+\frac{\mu_t}{\sigma_\epsilon})\frac{\partial\epsilon}{\partial x_j}\right]+C_{1\epsilon}\frac{\epsilon}{k}(G_k+C_{3\epsilon}G_b)-C_{2\epsilon}\rho\frac{\epsilon^2}{k}+S_\in \quad (7)$$

Where:

$$\mu_t=\rho C_m\frac{k^2}{\epsilon}, G_k=-\rho u'_i u'_j\frac{\partial u_j}{\partial x_i}, G_b=\beta g_i\frac{\mu_t\partial T}{Pr_t\partial x_i}$$

And, the Turbulent viscosity is μ_t, the effect of buoyancy is G_b the Rate of dissemination is Y_m, turbulent kinetic energy generation is G_k, and the Turbulent velocity is u', the coefficient of the thermal expansion is β, the turbulent Prandtl number is Pr_t, at default =0.85, the sours terms defined by used are S_k, $S_\in$and the reverse active prandtle are σ_ϵ, $\sigma_k$for ϵ, K respectively. Constants model at default value is:$C_{1\epsilon}$ =1.44,$C_{2\epsilon}$ =1.92,C_m =0.09,σ_k =1,σ_ϵ =1.3,$\sigma_{3\epsilon}$ =-0.33.

2.3 Combustion model

The probability density function (pdf) was used in this study to assess a few combustion parameters. A clipped Gaussian and a beta function are two different forms of probability density functions that can be derived from the mixture fraction to show the amounts of the conserved scalar that are impacted by the turbulence fluctuation. A beta function is frequently employed in the current study because of its simplicity and affordability. Mathematical identification of the beta function:

$$p(f)=\frac{f^{\psi-1}(1-f)^{B-1}}{\int_0^1 f^{\psi-1}(1-f)^{B-1}df} \quad (8)$$

$$f=\frac{z_i-z_{i,ox}}{z_{i,fuel}-z_{i,ox}} \quad (9)$$

Mathematical definitions of the explicit functions of (f,g)

$$\psi=\tilde{f}\left[\frac{\tilde{f}(1-\tilde{f})}{g}-1\right] \quad (10)$$

$$B=(1-\tilde{f})\psi \quad (11)$$

The temperature and enthalpy of each product's species concentration were calculated by weighing these values in accordance with (pdf) for the fraction of mixture $\tilde{p}$(f). The $\tilde{f}$,g computed for each grid using the finite difference technique, Q may be expressed

$$\tilde{Q}=\int_0^1 p\check{}\,(f)Q(f)df \quad (12)$$

where: $\tilde{Q}$ is the Favre-averaging quantity, a mixture fraction is $f, mean\ mixture\ fraction\ of\ mass$ is $\tilde{f}$ coefficients of beta pdf are B,ψ, the species element's mass fraction I am Z_i, Fuel stream input mass fraction is $Z_{i,fuel}$, and the mass percentage at the oxidizer stream inlet is $Z_{i,ox}$.

2.4 The P-1 Radiation Modelling

The P-1 radiation model is a condensed form of the P-N model, which expands the radiation intensity I into an orthogonal series of spherical harmonics. [27], (28). The equations utilized in the P-1 model are detailed in this section. See Using the Radiation Models for details on how to set up the model. The P-1 radiation model is the most basic version of the P-N model. If only four terms in the series are utilized to simulate gray radiation, the following equation is produced for the radiation flux:

$$q_r=\frac{1}{3(a+\sigma_s)-C\sigma_s}\nabla G \quad (13)$$

Where α is the absorption coefficient, σ_s is the scattering coefficient, G is the incident radiation, and C is the linear-anisotropic phase function coefficient, described below. After introducing the parameter.

$$\Gamma=\frac{1}{(3(a+\sigma_s)-C\sigma_s)} \quad (14)$$

Equation (2) simplifies to,

$$q_r=-\Gamma\nabla G \quad (15)$$

The transport equation for G is:

$$\nabla.(\Gamma\nabla G)-aG+4an^2\sigma T^4=S_G \quad (16)$$

Where σ is the Stefan-Boltzmann constant, n is the refractive index of the medium, and SG is a user-defined radiation source. This equation is solved by ANSYS FLUENT to produce the local incident radiation. When the P-1 model is in operation. Equation Combination (17) and Equation (18) yields the following equation:

$$-\nabla.q_r=aG-4an^2\sigma T^4 \quad (17)$$

The expression for - ∇. q_r may be used to directly account for heat sources (or sinks) caused by radiation in the energy equation. In order to simulate non-gray radiation using a gray-band model, Equation (18) is modified as follows:

$$\nabla.(\Gamma_\lambda\nabla G_\lambda)-a_\lambda G_\lambda+4a_\lambda n^2\sigma T^4=s_{g\lambda} \quad (18)$$

Where n is the medium's refractive index, a-(λ) is the spectral absorption coefficient, and G_λ is the spectrum of incident radiation, $_{SG\lambda}$ is a user-defined source term. Γλ Is defined as:

$$\Gamma_\lambda=\frac{1}{(3(a_{\lambda+\sigma_{s\lambda}})-C\sigma_{S\lambda})} \quad (19)$$

Where C is the coefficient of the linear anisotropic phase function and ($\sigma_{s\lambda}$)is a spectrum scattering coefficient. Black body spectral emission ($G_{b\lambda}$) between wavelength λ1 and λ2

$$G_{b\lambda}=4[F(0\to n\lambda_2 T)-F(0\to n\lambda_1 T)]\sigma T^4 \quad (20)$$

Where $F0 \rightarrow n\lambda$ is the portion of radiant energy that a black body emits in the wavelength range. The wavelength boundaries of the band are λ_1 and λ_2, and it ranges from 0 to λ at temperature T in a medium with refractive index n. The following formula is used to calculate the spectral radiative flux:2T

$$q_\lambda = -\Gamma \nabla G_\lambda \tag{21}$$

The energy equation's radiation source term is expressed as

$$-\nabla q_r = \sum_{AllBands} -\nabla q_{r,\lambda} = \sum_{allBands} a_\lambda (G_\lambda - n^2 G_{b\lambda}) \tag{22}$$

2.4.1 Liquid phase

It has been proposed that the liquid phase (discrete droplets) in the gas phase (continuous phase) is spherical. The model uses the Lagrangian approach to integrate the force balance to calculate the trajectory of liquid-phase droplets at the start of solutions. After the gas phase has been recalculated and modified, the liquid phase is solved in the following equation, and the governing equations are provided by [29]:

$$\frac{du_p}{dt} = f_D(u - u_p) + \frac{g_{x(\rho p - \rho)}}{\rho_p} + \frac{\rho}{\rho_p} u_p \frac{\partial u}{\partial x_i} \tag{23}$$

$$f_D = \frac{18\mu}{\rho_p d_p^2} \frac{c_D R_e}{24} \tag{24}$$

$$R_e = \frac{d_p \rho |u_p - u|}{\mu} \tag{25}$$

Where the droplets velocity is u_p in (m/s), the drag force effect per unit particle mass is $f_D(u - u_p)$ in $(m\ /s^2)$, the gravitational force effect on the droplet is ($\frac{g_{x(\rho p - \rho)}}{\rho_p}$). The third term on the right hand is an additional force created by the pressure gradient in the fluid. $\frac{du_p}{dt}$ Term denotes the evaporation rate of the particle. The gravity is g_x in ($m\ /s^2$), the droplet diameter is d_p, and the drag coefficient is C_D, and a_1, a_2, anda_3 can be defined as constants given by [30]. The heat balance for determining heat transfer between gas-phase and liquid-phase. Investigating the impact of the particles' drag force is one of the key factors. In order to character torag force coefficient (CD), drag correlation Morse and Alexander [30] is used, presuming that the droplet has a spherical shape.

$$CD = a_1 + \frac{a_2}{R_e} + \frac{a_3}{R_e^2} \tag{26}$$

Where:$a_1, a_2, and\ a_3$ are constants. The differential in vapor concentration between the gas phase and the droplet surface influences the rate of vaporization.

$$N_i = K_c (C_{i,s} - C_{i,\infty}) \tag{27}$$

$$K_c = \frac{S_h D_{i,m}}{d_p} = \frac{\left(2 + 0.6 R_e^{1/2} S_c^{1/3}\right) D_{i,m}}{d_p} \tag{28}$$

$$C_{i,\infty} = X_i \frac{P}{RT_\infty} \tag{29}$$

$$C_{i,s} = \frac{P_{sat}(T_p)}{R(T_p)} \tag{30}$$

where:N_i is the vapor molar flux in($kg\ mole/m^2\ s$),$C_{i,s}$ is the vapor concentration of the droplet surface in($kg\ mole/m^3$) , k_c is the coefficient of mass transfer in (m/s),$C_{i,\infty}$ is the concentration of vapor in the continuous phase in ($kg\ mole/m^3$), the local bulk mole fraction for a specific direction (i) denoted, the saturated vapor pressure is P_{sat} in (Pa), the universal gas constant is denoted R in(J/kg . k), Sherwood number is denoted (Sh), and Schmidt number is (Sc).In fluent Ansys Law, 2 is governing the droplet evaporation is identified as :

$$m_p(t + \Delta t) = mp(t) - N_i A_p M_{w,i} \Delta t \tag{31}$$

where the molecular weight at specific phase (i) is denoted by $M_{w,i}$, the droplet average mass in the control volume is $\bar{m}_p$ in (kg), the term of the volumetric source denoted by S_h, can be expressed as follows:

$$S_h = \left[\frac{\bar{m}_p}{m_{p,o}} cp \Delta T_p + \frac{\Delta m_p}{m_{p,o}} \left(-h_{fg} + \int_{T_{ref}}^{T_p} C_{p,i} dt\right)\right] \dot{m}_{p,o} \tag{32}$$

To solve the two connected stages, an iterative technique is used. The mass, heat, and momentum received or lost by the particle stream are determined after a particle route has been calculated. Following that, and accounted for in gas-phase calculations The mass transfer from the liquid phase to the solid phase. The mass fluctuations between the control volumes are used to determine gas-phase s_m. It is calculated using the following equations:

$$S_m = \frac{\Delta m_p \dot{m}_{p,o}}{m_{p,o}} \tag{33}$$

Where the particle mass change in each control volume is Δm_p, the initial mass flow rate of the particles is $m_{p,o}$, and the mass flow rate of particles is m_p. The exchanging mass is then used as a source of mass in the gas-phase and species equation's continuity equation. The change in a particle's momentum across control volumes may be used to represent the momentum transfer between two phases using:

$$F_i = \sum \left(\frac{18\mu}{\rho_p d_p^2} \frac{c_D R_e}{24} (u - u_p) + \frac{g_{x(\rho p - \rho)}}{\rho_p} + \frac{\rho}{\rho_p} u_p \frac{\partial u}{\partial x_i}\right) \dot{m}_p \Delta t \tag{34}$$

3. Numerical method

The Ansys Fluent software is used in this work. All the presented test cases, the finite volume approach is implemented. It is the most suitable numerical method for simulating two-phase flow. It is a discretization method for a system of partial differential equations that determines the balance or conservation of one or more quantities. These equations can be described as parabolic or elliptic, and they are used in a variety of domains including physics, chemistry, and dynamic reliability. The characteristics and flow variables as average values along a given control volume are found using the finite volume method in this study. It deals with the governing equations that are represented by the mass, momentum, and energy conservation laws. To maintain numerical stability, the pressure-velocity coupling equations are solved using the SIMPLE algorithm approach, with second-order upwind fitted to the scaler convection term in mean mixture fraction, momentum, kinetic turbulence energy, energy, and mixture fraction variance. The initial upwind approach was based on the turbulence dissipation rate. Figure1. (A) illustrates the spray combustor schematic.

It's a two-dimensional domain that represents an axisymmetric arrangement (1x10) m, under steady-state conditions. There is only one coflow in the domain. The temperature of the domain walls is maintained

at 296 k. The boundary condition at the top is set symmetry Figure 1. (B) depicts the two-dimensional structural grid's computational domain. The region adaption strategy is used in this research. It is appropriate for a specific solution domain region. A two-dimensional inside improvement of the quadrilateral is examined. The standard case, which delivers the best numerical simulation to the experimental data when compared without mesh, is reached after two cycles of adaption. The number of mesh has affected numerical results, as seen in figure 1. (C). As a result, three adoptions are employed. Using initial adaption (20800*42052*21253), some numerical results were obtained. As a second adaption, a higher mesh density (83200*167304*84105) is used in the next step. The outcome in this example differs from the initial adaption. The final adaption (83200*167304*84105) is then achieved by using a higher cell density. All numerical values obtained using the third adaption are comparable to those obtained using the second adaption. The numerous mesh generators create meshes with cell volumes that increase quickly as they get farther away from boundaries. While this naturally prevents a mesh from becoming too dense, it can become problematic if the mesh is not fine enough to stop the flow. Region adaptation can be used to refine the mesh if a finer mesh is required in a particular area of a solution domain. For places that demand high resolution, region adaption is particularly crucial. Two-dimension is used in this work. The computational domain employed in two situations is depicted in Figure (1). The results from the four levels of grid resolution are various in the three levels: coarse, medium, and fine. The best results shows in the third level (fine grid).

Table 1. The grid specification

Details	Coarse mesh	Medium mesh	Refine mesh
CELL	5200	20800	83200
Faces	10626	42052	167304
Nodes	5427	21253	84105

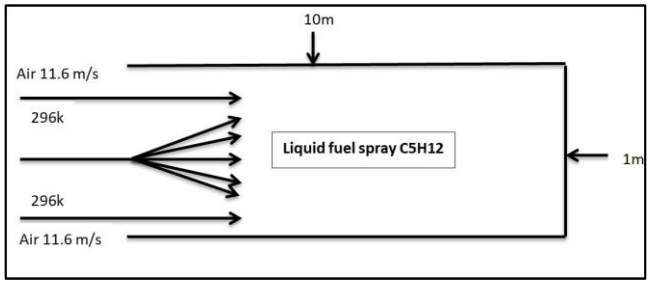

Figure 1. (A) The spray combustor schematic of the case1

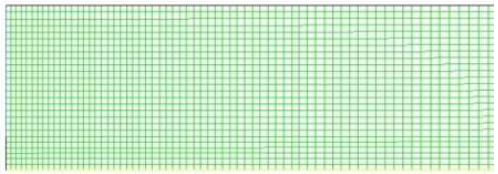

a-Coarse mesh

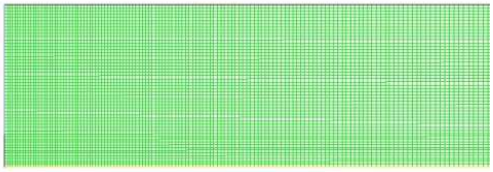

b-Medium mesh

c-Refine mesh

Figure 1. (B) The computational domain. Numerical values obtained using the third adaption are comparable to those obtained using the second adaption

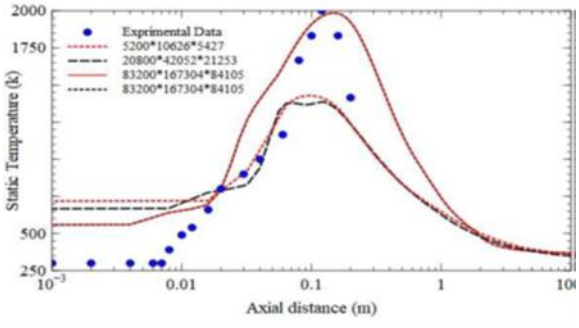

Figure 1. (C) Comparison between the adaption effects of prediction gas temperature with experimental data

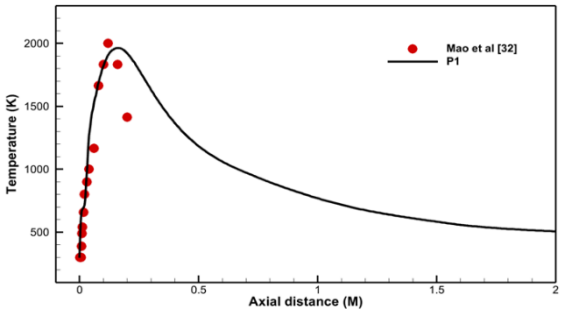

Figure 2. Comparison between calculated gas temperatures predicted by the p1 model and Mao et al [32]

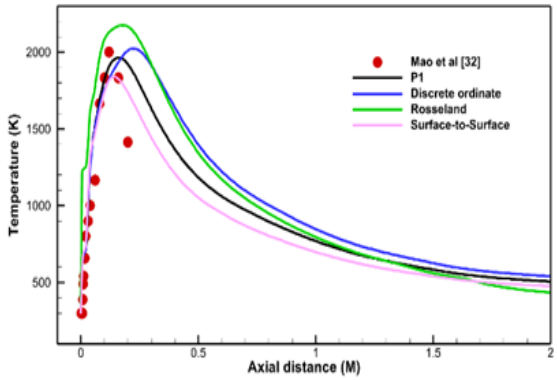

Figure 3. Comparison between calculated gas temperature predicted by p1, Discrete ordinate, Roseland, and Surface -to -Surface radiation model and Mao et al[32]

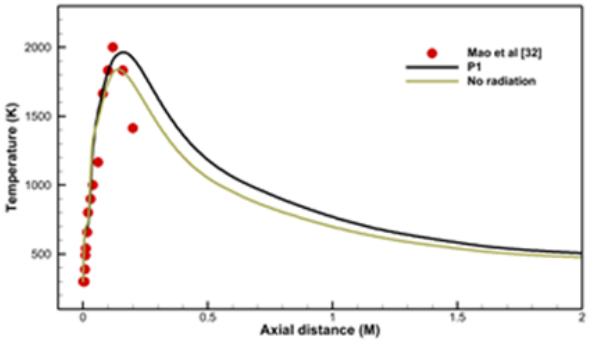

Figure 4. Comparison between calculated gas temperatures predicted by the p1 model, no radiation model, and Mao et al [32].

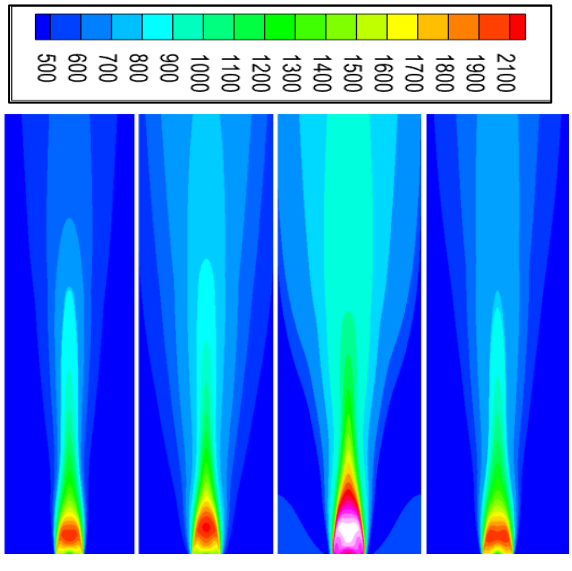

Figure 5. Contours plots of gas temperature at different radiation models

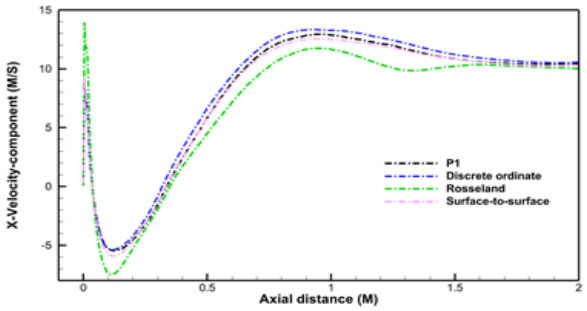

Figure 6. X-velocity profiles of the gas phase at different radiation models along the centerline

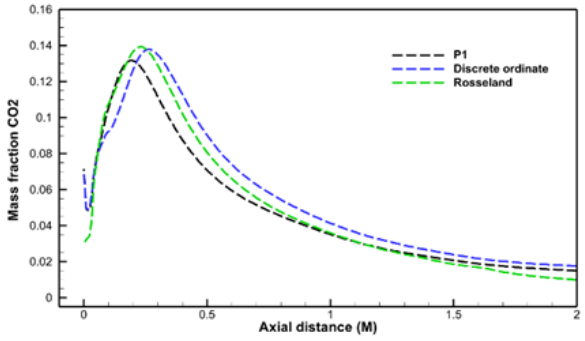

Figure 7. Mass fraction (CO2) profiles of the gas phase at different radiation models along the centerline.

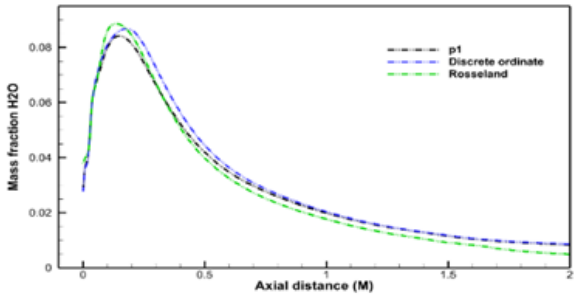

Figure 8. Mass fraction (H2O) profiles of the gas phase at different radiation models along the centerline.

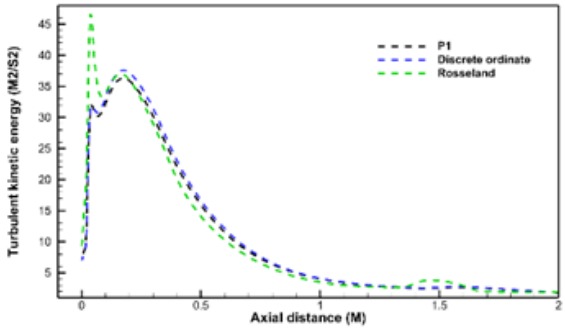

Figure 9. Turbulent kinetic energy profile of the gas phase at different radiation models the centerline.

4. Results and discussions

The injection conditions of the spray droplets are taken from Mao et al [32]. Figure 2, shows a comparison between the gas temperature and Mao et al [32]. The Numerical solution of spray combustion using the p1 model gives an approximate trend with measured results. Figure 3, shows a comparison between the static temperatures for the four radiation against Mao et al [32]. And show results on P1 and Discrete Ordinate model best from another models. Figure 4, shows a comparison between the static temperature for the P1radiation model and no radiation against Mao et al [32]. These profiles are reaching maximum values near the nozzle region due to hydrodynamic and chemical reactions between the two phases. It can be noticed that the p1 radiation model has a very close trend compared with Mao et al [32]. The difference between the Mao et al [32] and numerical simulation is recorded as 0.9% of the P1- results, 1.0% of the discrete ordinate, 6%surface- to surface, and 7% for the Roseland model. Figure 5, shows the contour plots for the gas static temperature for four different radiation models. It can be seen that the discrete ordinate model gives a good resolution but it is far away from Mao et al [32].While the p1 model is demonstrating more stability among the four models. Figure 6, shows the x- velocity component of the gas phase along the centerline. The decay in the x-velocity component of the gas phase is a result of the evaporation process for the droplet near the nozzle orifice and then returns to raise due to a reduction in the density of the gas. At $0< x< 10$ cm, each discrete ordinate, Roseland, and surface-to-surface radiation model along with axial distance coincide at a specific region and then diverge. While the p1 model exhibits separate behavior as compared with the discrete ordinate, Roseland, and surface-to-surface models. At x=10 cm four models reach minimum levels of velocity. At $x > 10$ cm when the spray droplets are combusting, it converts to a single phase. The x-velocity component tends to increase again and converge approximately for the four radiation models. Figure7, when radiation models are considered, CO2 in the P1 model is reduced from discrete ordinate and Roseland As it is seen, the radiation effect of the gray gases of CO2 changes the species mass fractions, and the results improve. Figure 8, when radiation models are considered, H2O in the p1 model is reduced from discrete ordinate and Roseland as it is seen, the radiation effect of the gray gases of H2O changes mass fractions, and the results improve. Figure 9, shows the turbulent kinetic energy profiles of the gas phase at different radiation models along the centerline. The Rosseland model is expressed with a large build-up of the radiation field and distributed near the nozzle region during an interaction between the liquid phase and gas phase. Then is deniedny downstream as it is far away from the nozzle. The surface-to-surface model gives the same induction but with a low level of intensity.

5. Conclusions

The four radiation models are used (P1, Discrete ordinate, Roseland, and Surface to Surface) for simulating the 2-D steady-state spray combustion. The work is based on comparisons among the radiation models. The numerical simulations are validated with available work by Mao et al. [32]. The investigation of the behavior of steady-state spray combustion at various radiation models with typical different parameters such as static temperature, gas phase velocity components, mass fraction CO2, mass fraction H2O, and turbulence kinetic energy. The P1 radiation model gives a better agreement with Mao et al. While the (Rosseland, Surface-to-Surface) radiation model has limitations that make it difficult to converge with Mao et al [32], The Discrete ordinate model shows a good prediction of the distribution of turbulence energy due to its accuracy in capturing rapid strained flow. It can be concluded that the P1 radiation model may be used to stimulate spray combustion with a minimum cost of computer energy and maintain realistic consideration. In the end, we can say that the P1 radiation model is the best for a spray combustion flame out of the four models.

Authors' contribution

All authors contributed equally to the preparation of this article.

Declaration of competing interest

The authors declare no conflicts of interest.

Funding source

This study didn't receive any specific funds.

REFERENCES

[1] Sikic, Dembele, S. Wen, Non-grey radiative heat transfer modeling in LES-CFD simulated methanol pool fires. *Journal of Quantitative Spectroscopy and Radiative Transfer, 234* (2019) 78-89.

[2] R. Siegel, J. R. Howell, *Thermal Radiation Heat Transfer*, McGraw Hill New York, (1993)

[3] T. DN, Modeling of 3-D non-gray gases radiation by coupling the finite volume method with weighted sum of gray gases model, Int J Heat Mass Transfer, 47 (2004) 1367–82.

[4] T. DN, O. TJ, A. CH, Modeling the radiation of anisotropically scattering media by coupling Mie theory with finite volume method, Int J Heat Mass Transfer, 47(26) (2004) 5765–80.

[5] Y. Sun et al, One-dimensional P1 method for gas radiation heat transfer in spherical geometry, International Journal of Heat and Mass Transfer, 145(2019) p. 118777.

[6] C. Yin, Nongray-gas effects in modeling of large-scale oxy-fuel combustion processes, Energy and Fuels 26 (2012) 3349e3356.

[7] A.A. Gamil et al. , Assessment of numerical radiation models on the heat transfer of an aero-engine combustion chamber, Case Studies in Thermal Engineering, 22 (2020) p. 100772.

[8] S. W. Baek., J. H. Park, C. E. ,Choi Investigation of droplet combustion with nongray gas radiation effects. *Combustion science and technology*, *142*(1-6) (1999) 55-79.

[9] S. Hjärtstam, R. Johansson, K. Andersson, F. Johnsson, Computational fluid dynamics modeling of oxy-fuel flames: the role of soot and gas radiation, Energy and Fuels 26 (2012) 2786e2797.

[10] M.K. Denison, A spectral line-based weighted-sum-of-gray-gases model for arbitrary RTE solvers, Ph.D. Thesis,Brigham Young University, Provo, UT, 1994.

[11] C. E. ,Beak SW, Numerical analysis of a spray combustion with non gray radiation using weighted sum of gray gases model, J Combust Sci Technol, 115 (1996) 297–315.

[12] E.E. Fordoei, K. Mazaheri, A. Mohammadpour, Effects of hydrogen addition to methane on the thermal and ignition delay characteristics of fuel-air, oxygen-enriched and oxy-fuel MILD combustion, International Journal of HydrogeEnergy, 46(68) (2021) p. 34002-34017.

[13] A. Frank, W. Heidemann, K. Spindler, Modeling of the surface-to-surface radiation exchange using a Monte Carlo method, Journal of Physics: Conference Series, (2016) 745.

[14] A.A. Hosseini, Numerical study of inlet air swirl intensity effect of a Methane-Air Diffusion Flame on its combustion characteristics, Case Studies in Thermal Engineering, 18 2020 p. 100610.

[15] P. Tóth, C. Brackmann, Y. Ögren, , M. N. Mannazhi, J. Simonsson, A. Sepman, H. Wiinikka, Experimental and numerical study of biomass fast pyrolysis oil spray combustion: Advanced laser diagnostics and emission spectrometry, Fuel, 252 (2019) 125-134.

[16] G. Krishnamoorthy A computationally efficient P1 radiation model for modern combustion systems utilizing pre-conditioned conjugate gradient methods. Applied Thermal Engineering, 119 (2017) 197-206.

[17] P. Crnjac, Implementation of the Rosseland and the P1 radiation models in the system of Navier-stokes equations with the boundary element method, International Journal of Computational Methods and Experimental

Measurements, **5**(3) (2017) p. 348-358.
[18] F. Jurić, , Z. Petranović, , M. Vujanović, , N. Duić, Numerical assessment of radiative heat transfer impact on pollutant formation processes in a compression ignition engine, Journal of Cleaner Production, 275 (2020) 123087.
[19] T. Furuhata, S. Tanno, T. Miura, Y. Ikeda, T. Nakajima, Performance of numerical spray combustion simulation, Energy conversion and management, 38(10-13) (1997) 1111-1122.
[20] Z. Yue, R. D. Reitz, Numerical investigation of radiative heat transfer in internal combustion engines, Applied Energy, 235 (2019) 147-163.
[21] C. Aghanajafi , A. Abjadpour, Discrete ordinates method applied to radiative transfer equation in complex geometries meshed by structured and unstructured grids, Journal of the Brazilian Society of Mechanical Sciences and Engineering, 2015. 38.
[22] S. Bellan, et al., Numerical and experimental study on granular flow and heat characteristics of directly-irradiated fluidized bed reactor for solar gasification, International Journal of Hydrogen Energy, 43(34) 2018 p. 16443-16457
[23] M. Rajhi, et al., *Evaluation of gas radiation models in CFD modeling of oxy-combustion.* Energy conversion and management, 2014. 81: p. 83-97.
[24] H. Watanabe, Y. Suwa, Y. Matsushita, Y. Morozumi, H. Aoki, S. Tanno, Spray combustion simulation including soot and NO formation, Energy Convers Manage;48 (2007) 2077–89.
[25] M. Bidi, M. Nobari, M. Saffar, A numerical investigation of turbulent Premixed methane–air combustion in a cylindrical chamber, Combust Sci Technol, 179 (2007) 1841–65.
[26] M. A. Chishty, M. Bolla, E. Hawkes, Y. Pei, S. Kook, Assessing the importance of radiative heat transfer for ECN Spray A using the transported PDF method, SAE International Journal of Fuels and Lubricants, 9(1) (2016) 100-107.
[27] R. Siegel, J. R. Howell, Thermal Radiation Heat Transfer, Hemisphere Publishing Corporation,Washington DC. 1992.
[28] P. Cheng, Two-Dimensional Radiating Gas Flow by a Moment Method, AIAA Journal. 2. 1662–1664.
[29] S. Pope, Combustion Modelling using Probability Density FunctionMethods, Numerical Approaches to Combustion Modelling, Prog. Astronaut. Aeronaut, AIAA, 1991.
[30] S. Morsi , A. Alexander , An investigation of particle trajectories in two-phase 208 systems, Journal of Fluid mechanics, vol. 55, no. 2, pp. 193- 208, 1972.
[31] H. K. Versteeg, W. Malalasekera, An introduction to computational fluid Dynamics: the finite volume method. Pearson education, 2007
[32] C.-P.Mao, G. Szekely Jr, G. Faeth, Evaluation of a locally homogeneous model of spray combustion, Journal of Energy, vol. 4, no. 2, pp.78-87, 1980.